

---

## Investigation and optimisation of cracked aluminium alloy plate restored for fatigue loading application

---

S. Tamboli\* and A. Pandey

Department of Mechanical Engineering,  
Symbiosis Institute of Technology,  
Symbiosis International University, India

Email: shahidt@sitpune.edu.in

Email: anand.pandey@sitpune.edu.in

\*Corresponding author

Mukundraj V. Patil

Intelligent Artificial Machine for Computing,  
Optimization and Learning,  
Pune, India

Email: mukundrajpatil@gmail.com

**Abstract:** Crack propagation could be catastrophic, and it needs the urgent attention of the user. A cracked structure needs to be repaired or replaced at the earliest. Costs associated with the complete replacement of the part paves the way for the former option, especially in the aircraft industry. Composite materials have good directional properties in the strength and toughness compared to the conventional materials like metals, alloys and plastics. In this study carbon fibre reinforced polymer (CFRP) has been used to repair the inclined crack in aluminium alloy plate having 1.6 mm thickness. Repaired aluminium alloy specimens were subjected to fatigue load to investigate the effectiveness of CFRP. By using the ply drop technique, the strength of the damaged structure has been restored. Various options have been evaluated by conducting the design of experiment. A peeling off tendency of the CFRP patch was observed during the study. To suppress this peeling off tendency, interfacial shear stress between CFRP and the aluminium was studied more intensely rather than the fracture toughness parameters. To select the optimum configuration MCDM optimisation techniques were used and numerical solutions were validated by lab experiments.

**Keywords:** CFRP material; crack repair; interfacial shear stress; peeling of tendency; multi-criteria optimisation; finite element analysis.

**Reference** to this paper should be made as follows: Tamboli, S., Pandey, A. and Patil, M.V. (2022) 'Investigation and optimisation of cracked aluminium alloy plate restored for fatigue loading application', *Int. J. Computer Aided Engineering and Technology*, Vol. 16, No. 2, pp.153–169.

**Biographical notes:** S. Tamboli is working as an Assistant Professor in the Department of Mechanical Engineering, Symbiosis Institute of Technology. He has ten years of teaching experience. He obtained his MTech from the COEP, Pune. His area of interest includes composite materials, fracture mechanics, optimisation algorithms and finite element analysis.

A. Pandey is a retired Colonel. At present he is working as the Head at the Mechanical Engineering Department, Symbiosis Institute of Technology. He served in the Indian army and worked on many reputed projects. He obtained his PhD from the COEP, Pune. His area of interest includes composite materials, IC engines, e-mobility and bio-fuels.

Mukundraj V. Patil received his PhD in the Domain of Multi-Objective Optimisation in 2021. He is an expert in multi-objective optimisation, meta-heuristics design, swarm and evolutionary intelligence, multi-criteria decision making, engineering optimisation, data visualisation, design of experiments, etc. He is a member of Multiple Criteria Decision Making (MCDM) and International Quality Federation (IQF) societies. Also, he is a reviewer of leading refereed international journals in his area of expertise.

---

## 1 Introduction

Airplane structures like wings surfaces are frequently subjected to stress reversals that results into cracks. In such a case, the remedy is to either restore or replace the structure. Restoration of a cracked structure is always preferable instead of its replacement since higher cost is involved in the latter approach as compared to the former approach. It is important to note that the restoration needs to be performed with due care following the International standards code for trust worthy results (Eliasson et al., 2019). Effectiveness of the restoration approach is ensured when necessary simulation tests are performed. New research trend of utilising composite materials in aircraft restoration began in Aeronautical and Maritime Research Laboratory, Australia (Baker, 1987). Since then, researchers are exploring various alternative solutions of the composite materials in the field of crack restoration. In another study, multiple comparisons between composite and metallic patches were performed to study the restoration effectiveness and it was found that the composite patch offers significant reduction in the stress intensity factor (SIF) (Bachir Bouiadjra et al., 2015).

The study of crack propagation and prevention of its growth is the subject of fracture mechanics. Parameters responsible for fracture toughness such as 'J' integral (J), SIF (K), and energy release parameters (G) were developed by the researchers to evaluate crack propagation (Rice, 1967; Vavrik and Jandjsek, 2014). In fact, the use of fracture toughness parameters and the standard procedure adopted for linear-elastic and elastic-plastic fracture mechanics was compiled by the researchers (Zhu and Joyce, 2012). This approach is well suited when the repairing is performed using fasteners and rivets. However, when the repairing is performed using adhesively bonded composite material, altogether different approach is required. The major hurdle in crack repair using the composite material is their tendency to debond from the cracked structure leading to the failure of a whole structure. In order to prevent debonding of composite materials in repaired metallic sheets, geometrical aspects of the patch were studied using FEA (Papanikos et al., 2007). Similarly, in another study of composite materials, the role of adhesive thickness was investigated (Moradi et al., 2013; Ouinas et al., 2012). It was observed that some researchers focused their attention on improving fracture toughness

of the repaired structure. Usually, it is preferable to apply patch on both the sides of a structure, as it offers balancing of the mass (Srilakshmi et al., 2015). However, it is not possible to apply patch on both the sides of a complex structure in which the other side is not accessible due to space or design limitation. In such cases, one-sided repair is applied. Another parameter of interest in the study of crack prevention is the ply thickness. The effect of different ply thicknesses used in composite laminate structure subjected to repeated loading was studied for damage prevention (Ali et al., 2020). Palm leaf stalks were hybridised with glass fibres prior to reinforcement in the polyester resin matrix. After studying the tensile strength as the response the combination was recommended to manufacture components like car bonnets and bumpers (Raj et al., 2021). More SIF was observed in a single sided repair than the double sided one. In case of single sided repair, transversely graded material and unbalanced lamina reduced the SIF to the considerable extent (Ramji and Srilakshmi, 2012). Mixed mode tensile loading was studied for inclined crack and optimum CFRP configuration was suggested (Tamboli et al., 2019). 60% carbon fibre reinforced with alumina and molybdenum disulfide fillers gave better mechanical properties (Suresha and Saini, 2018). Glass – carbon/epoxy hybrid composites were tested against the low velocity impact. This study concluded that defect in these composites has significant effect on energy absorption during the impact (Venkategowda et al., 2018). For fatigue application of the composite material, Kevlar-49 was chosen as the fibre material whereas cork powder and nanoclays were used to improve the impact resistance and tensile strength of these laminates (Kaliraj et al., 2017). In one of the application aluminium metal matrix composites were prepared by in-situ method and tested for hardness, tensile strength and microstructure (Mohan et al., 2018). In another study varying percentage of resin was used to prepare glass wool reinforced composite and its properties were evaluated. It was found that 40% glass wool gives better strength (Thirukumaran et al., 2018). Researchers also studied patch shape, size and sequence effect on repair efficiency (Pandey and Kumar, 2010). Titanium oxide (TiO<sub>2</sub>) (5 wt.%), alumina oxide (AO) (10 wt.%) and silicon carbide (SC) (5 wt.%) reinforced Nylon 6 (N6) composites gear were manufactured for industrial and automobile applications (Vignesh and Kumar, 2022). This improved the tensile properties and thermal stability of the N6 polymer matrix composites. To minimise the impact on environment and explore the renewable option in composite materials natural fibres from rice husks, saw dust, cashew nut shells were used in the composite manufacturing and their mechanical properties were tested (Saravanan and Ganesan, 2017).

For selecting the optimum parameters of TIG welding response surface methodology was used to minimise the bead width, height and maximise the depth of penetration (Srivastava et al., 2021). ‘Analytic hierarchy process (AHP) and technique for order preferences by similarity to ideal solution (TOPSIS)’ were used to analyse the material performance of SC reinforcement over AA 2024 alloy composite (Bhaskar et al., 2020). Fracture toughness properties like tensile strength, density and inter-laminar shear strength were optimised using TOPSIS for nanofiller composite. Mechanical, chemical, physical and thermal properties were optimised using AHP and ‘multi-objective optimisation based on ratio analysis’ (MOORA) (Maharana et al., 2020). MOORA technique was used to determine the process parameters like pulse on time, voltage and wire feed rate, metal removal rate and surface roughness for aluminium (A6061) reinforced zinc oxide particle metal matrix (Sadhasivam et al., 2021). Alternative

approach of response surface method of experimental design was also used for optimisation (Gangwar et al., 2021; Patil, 2017). It has been observed that researchers focused over optimising fracture toughness and other properties in the field of material science. Moreover, one or more optimisation methods has been used. However, it has been observed that the combination of TOPSIS, MOORA and vlskriterijumska optimisacija i kompromisno resenje (VIKOR) has not been used in the multi-criteria optimisation of CFRP and aluminium alloy for strengthening the bonding between them.

Based on the literature reviews performed so far, it has been observed that these studies focused much of their attention on reducing the fracture toughness parameters and paid little or no attention on reducing the debonding tendency between a parent material and a patch material. Moreover, mechanical structures are often subjected to a mixed mode of crack growth in the presence of tensile as well as fatigue load. Considering the critical nature of fatigue load on aircraft structures especially the wings, this study focused its attention on repair of cracked aluminium alloy by CFRP for fatigue loading. In this study it was found that interfacial shear stress is the principal cause for debonding between carbon fibre reinforced polymer (CFRP) and aluminium alloy plate. Therefore, the objective of this study was to minimise the interfacial shear stress and its fluctuation between CFRP and cracked aluminium alloy plate.

In this regard the novel contribution of this work are:

- 1 design and development of fatigue testing machine for rectangular specimen
- 2 focus on interfacial shear stress instead of fracture toughness parameters
- 3 three layers of ply thicknesses in different combinations to study the debonding phenomenon
- 4 experimental and physical simulations by finite element analysis and fatigue testing machine
- 5 use of multi-criteria optimisation techniques for finding out the optimum CFRP configuration.

## **2 Methodology**

In this study, the mixed mode of crack propagation has been studied from the perspective of suppression of CFRP's peeling off tendency from aluminium alloy plate. Figure 1 shows the flow of the work for this study. This study has been carried out by considering numerical as well experimental aspects.

### *2.1 Experimental setup*

#### *2.1.1 Machine setup*

Since the existing fatigue testing machines were able to accommodate only circular specimens, a new fatigue-testing machine was designed and developed in the research laboratory. Figure 2(a) shows the experimental setup whereas Figure 2(b) shows the repaired specimen which can be mounted at the designated place on a fatigue-testing machine.

Figure 1 Flow of the work (see online version for colours)

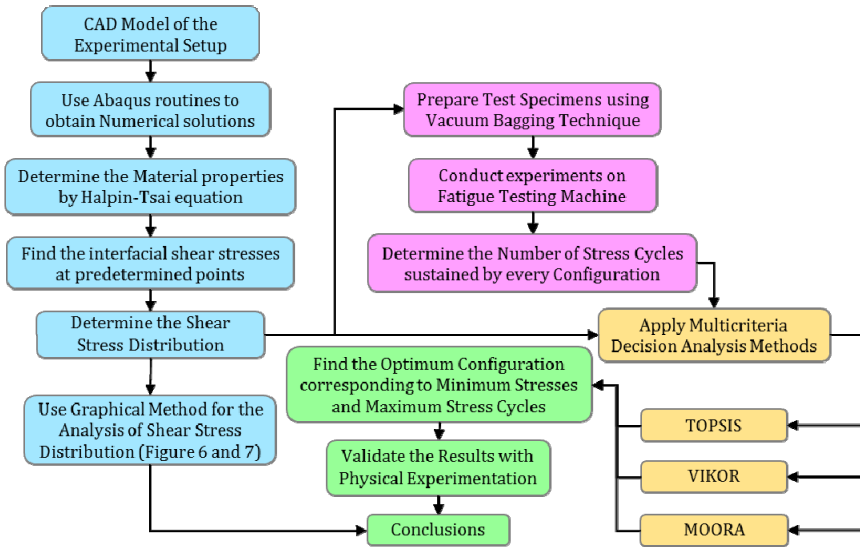


Figure 2 (a) Experimental setup (b) Repaired specimen (see online version for colours)

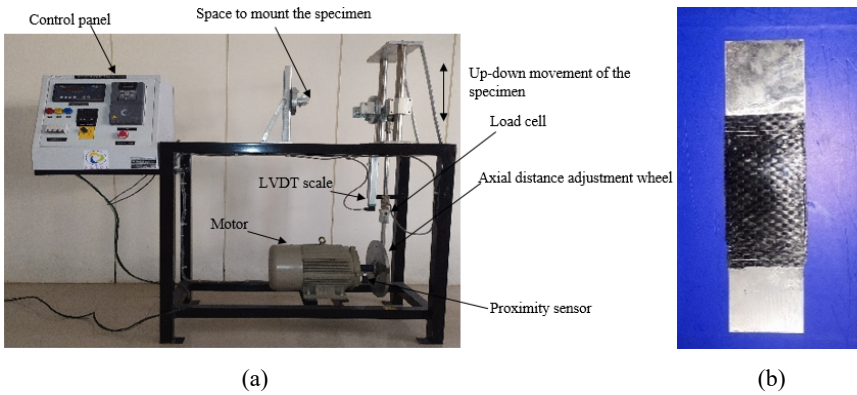
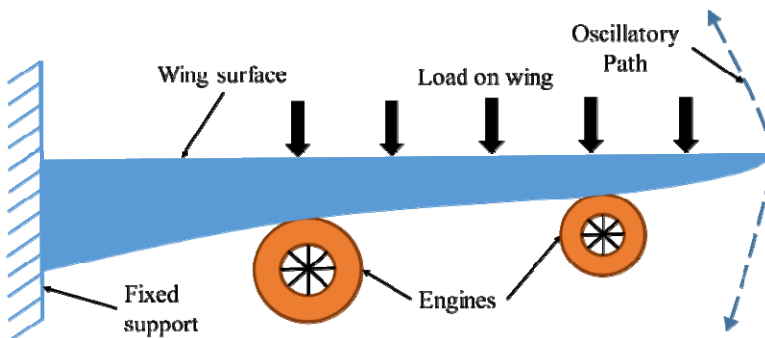


Figure 3 Oscillatory load on an aircraft wing (see online version for colours)



Wings of the aircrafts are generally subjected to fatigue loadings. The action of fatigue loading results into oscillatory motion of the wing about a fixed support as shown in Figure 3. This fatigue load consists of wind load as well as weight load of the engines. This movement of the wing was replicated on the fatigue testing machined shown in Figure 2(a) as well as in the finite element analysis.

### 2.1.2 Preparation of specimen for fatigue loading

An inclined crack was created in the middle region of the plate as shown in Figure 4(a) to ensure the presence of a mixed mode of crack propagation. The plate length, width and thickness were taken as 300 mm, 60 mm and 1.6 mm respectively. Figure 4(b) shows the side view of the geometry wherein three layers of CFRP are applied on one side of the cracked plate using ply drop technique. Three different types of CFRP fibre having different densities were used. It is important to note that 200 gsm CFRP represents low density, 300 gsm CFRP represents medium density, whereas 600 gsm CFRP represents high density. Varying the material density is requisite part of the experiment for suppressing the peeling off tendency of the CFRP material from the aluminium alloy plate.

**Figure 4** (a) Geometry of cracked specimen (b) Repaired specimen with three different GSM (see online version for colours)

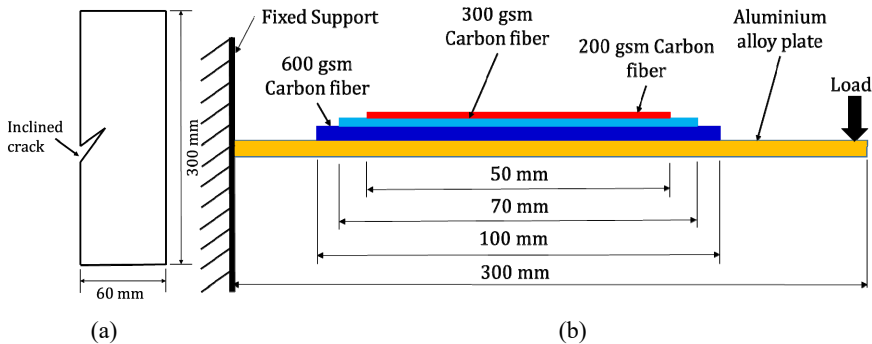


Figure 4(b) shows that the first CFRP fibre has a density of 600 gsm, whereas second and third fibre have densities of 300 and 200 gsm respectively. In every trial of the design of experiment, the fibre gsm sequence was changed but the CFRP length was kept constant as 100 mm, 70 mm and 50 mm for first, second and third ply positions respectively. This technique is known as a ply drop technique. Variation in the sequence of different material density resulted into the full factorial design of experiment with three levels of densities. By changing the sequence of the CFRP fibres, 27 different configurations were generated and evaluated. These configurations are discussed in 'result and discussion' section. CFRP exhibits peeling off tendency from the aluminium alloy. Aluminium alloy plate transfers the load to CFRP through interfacial shear stress between them and this is the main reason of peeling off tendency of CFRP. Because of this reason minimisation of shear stress and its fluctuation were focused on in this study rather than the fracture toughness.

### 2.1.3 Experimental data collection

With the help of vacuum bagging technique, 27 different specimens were prepared and tested on the fatigue testing machine (Cloud, 2016). The oscillatory movement of an airplane wing was simulated in the lab environment on repaired specimens using an 'axial distance adjustment wheel' shown in Figure 2(a). This wheel controls the range of displacement to be given to the specimen. Displacement was given to both side of a mean position. Load cell calibrates the displacement to the applied load. Linear variable differential transformer (LVDT) scale is used to capture the displacement with reference to the mean position of a wing. Proximity sensor captures the number of cycles the specimen is subjected in the experiment. This data is given to the feedback mechanism which analyses the load and number of cycles for a particular experiment. The CFRP configuration that sustained the greatest number of cycles was selected as the best configuration to sustain the fatigue loading environment.

## 2.2 Numerical analysis

With two objectives involved in this study, the numerical analysis was performed using Abaqus 6.14 software. In order to generate a mixed mode of crack propagation, an inclined crack was created in an aluminium alloy plate. To simulate the fatigue loading and increase the stress on the repaired structure, displacement was given on both the sides of a mean position. As shown in Figures 3 and 4(b), the base was constrained in all directions which acted as a sturdy fuselage of the aircraft. A fatigue load was applied at the tip of the plate in such a way that the plate was displaced at both the sides. In all 27 different configurations were simulated to observe interfacial shear stress and its fluctuation. The data obtained in this way was utilised for multi-criteria optimisation.

### 2.2.1 Material properties

Analytical relations for determining material properties were defined by the Halpin-Tsai equations (Patterson and Force, 1976). These equations help in obtaining material properties such as: longitudinal, transverse and shear modulus as well as Poisson's ratio [equations (1) to (4)]. Determining these engineering constants is very important, since CFRP is an orthotropic material which exhibits different constants in different directions.

Longitudinal modulus  $E_L$  is given by

$$E_L = E_f V_f + E_m V_m \quad (1)$$

where letter  $E$  and  $V$  stands for modulus of elasticity and volume fraction, whereas subscript  $f$  and  $m$  is used for fibre and resin.

Transverse modulus  $E_m$  is given by

$$\frac{E_T}{E_m} = \frac{1 + \zeta \eta V_f}{1 - \eta V_f} \quad (2)$$

whereas shear modulus is given by

$$\frac{G_{TL}}{G_m} = \frac{1 + \zeta \eta V_f}{1 - \eta V_f} \quad (3)$$

where  $\eta = \frac{\frac{E_f}{E_m} - 1}{\frac{E_f}{E_m} + \zeta}$  and  $\zeta$  is a constant.

Poisson’s ratio can be calculated by

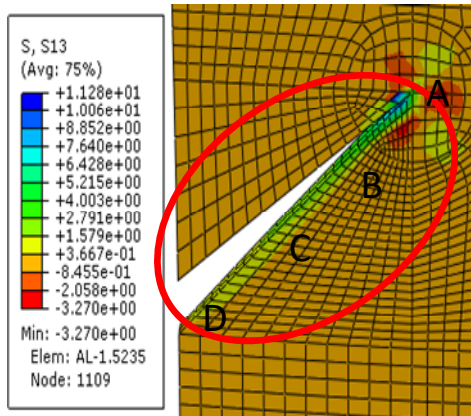
$$v_{LT} = v_f V_f + v_m V_m \tag{4}$$

In these equations,  $\zeta$  is a measure of reinforcement and depends on the geometry of carbon fibre and the type of loading. Halpin-Tsai suggested a value of  $\zeta = 2$  for fibre with circular cross section. Engineering constants calculated by above equations are shown in Table 1.

**Table 1** Engineering constants for CFRP

Engineering constants	Values
1 Longitudinal modulus in direction 1, E1 (GPa)	92.270
2 Young’s modulus in direction 2, E2 (GPa)	8.460
3 Young’s modulus in direction 3, E3 (GPa)	8.460
4 In-plane modulus of rigidity G12 (GPa)	2.593
5 Out of plane modulus of rigidity G13 (GPa)	2.593
6 Out of plane modulus of rigidity G23 (GPa)	1.370
7 Major in-plane Poisson’s ratio, $v_{12}$	0.290
8 Major out of plane Poisson’s ratio, $v_{13}$	0.290
9 Major out of plane Poisson’s ratio, $v_{23}$	0.400

**Figure 5** Critical area for the interfacial shear stress analysis (see online version for colours)



2.2.2 Numerical results analysis

Experiments were carried out in Abaqus 6.14 as well as in laboratory to find out the best configuration which would suppress the debonding tendency of the CFRP patch. In all, 27 different configurations were simulated in Abaqus by changing the CFRP’s gsm. In

this design of experiment interfacial shear stress was recorded for each specimen at the critical areas in numerical analysis whereas the specimen prepared according to these 27 configurations were tested on fatigue testing machine and the maximum loading cycles were observed against the first sign of delamination.

For the fatigue loading crack surface emerged as the critical area where high value of interfacial shear stress was observed at point A, B, C and D as shown in Figure 5. Figure 5 shows the interface between aluminium alloy plate and the first CFRP ply.

### 3 Multiple criteria optimisation

Multi-criteria optimisation is one of the approach of optimising multiple criteria (objectives), all at a time. In multi-criteria optimisation, choosing an optimum alternative is always challenging because of conflicting nature and multiple presence of criteria involved in the study (Patil and Kulkarni, 2020). Multiple criteria optimisation is also known as ‘multi-criteria decision making’ (MCDM). It is important to note that all the criteria of minimisation type are converted into maximisation type before applying the following MCDM procedures. Three different MCDM approaches used in this study are described in the following Subsections 3.1 to 3.3.

#### 3.1 TOPSIS

‘Technique for order of preference by similarity to ideal solution’ (TOPSIS) algorithm is presented below (Hwang and Yoon, 1981). It is one of the popular algorithm that provides the Pareto optimal solution which is nearest to ‘positive ideal solution’ (PIS) and farthest to ‘negative ideal solution’ (NIS).

Step 1 In the beginning, construct the decision matrix  $D$ . Normalise it using equation (5). First, perform the ‘max’ normalisation to avoid the scaling effect, then perform vector normalisation to distribute all the vectors uniformly in the range [0, 1].

$$v_{ij} = \frac{a_{ij}}{\sqrt{\sum_{i=1}^n a_{ij}^2}} \quad i = 1, \dots, n; j = 1, \dots, m \quad (5)$$

Step 2 Identify PIS and NIS solutions from  $V$ , represented as  $V^+$  [equation (6)] and  $V^-$  [equation (7)] respectively.

$$V^+ = \max \{v_1, \dots, v_j, \dots, v_m\} \quad (6)$$

$$V^- = \min \{v_1, \dots, v_j, \dots, v_m\} \quad (7)$$

Step 3 Determine distance of each vector from PIS and NIS using Euclidean norm [equations (8) and (9)].

$$d_i^+ = \left( \sum_{j=1}^m (v_{ij} - V^+)^2 \right)^{1/2} \quad (8)$$

$$d_i^- = \left( \sum_{j=1}^m (v_{ij} - V^-)^2 \right)^{1/2} \tag{9}$$

Step 4 Find out the relative distances of each distance vector from NIS solution [equation (10)].

$$S_i = \frac{d_i^-}{d_i^- + d_i^+} \tag{10}$$

Step 5 Arrange all the relative distances in the decreasing order. The highest distance value represents the first ranked solution.

### 3.2 VIKOR

VIKOR (Opricovic and Tzeng, 2004) method is similar to TOPSIS method, however, different in selecting the compromise solution. Normalisation is not the part of this procedure. Similar to TOPSIS, the normalisation of the decision matrix is proposed here to keep uniformity in the final result assessment.

Step 1 Determine the best  $f_i^*$  [equation (11)] and the  $f_i^-$  [equation (12)] performance values for each criterion.

$$f_i^* = \max_j f_{ij} \tag{11}$$

$$f_i^- = \min_j f_{ij} \tag{12}$$

Step 2 Find  $S_j$  and  $R_j$  for each criteria ( $j = 1, \dots, m$ ) using the equations (13) and (14).

$$S_j = \sum_{i=1}^n (f_i^* - f_{ij}) / (f_i^* - f_i^-) \tag{13}$$

$$R_j = \max_i [(f_i^* - f_{ij}) / (f_i^* - f_i^-)] \tag{14}$$

Step 3 Find  $Q_j$  values for each criteria ( $j = 1, \dots, m$ ) using the equation (15).

$$Q_j = v \frac{(S_j - S^*)}{(S^- - S^*)} + (1 - v) \frac{(R_j - R^*)}{(R^- - R^*)} \tag{15}$$

$v(0 < v < 1)$  is the weight factor which determines the type of strategy like maximum group utility. The usual value  $v = 0.5$  is used in this analysis.

Where

$$S^* = \min_j S_j \tag{15.1}$$

$$S^- = \max_j S_j \tag{15.2}$$

$$R^* = \min_j R_j \tag{15.3}$$

$$R^- = \max_j R_j \tag{15.4}$$

Step 4 Arrange  $S$ ,  $R$  and  $Q$  in the decreasing order to produce three ranking lists.

Step 5 Select alternative  $a_1$  (first rank) as the best alternative, if following conditions are met.

*Condition 1:* Acceptable advantage [equation (16)]

$$Q(a_2) - Q(a_1) \geqslant DQ \tag{16}$$

where  $a_2$  is the second best alternative.

$$DQ = 1/(m - 1) \tag{16.1}$$

*Condition 2:* Acceptable stability.

An alternative  $a_1$  should be ranked by  $S$  and/or  $R$  under influence of any one of the strategy: voting by majority ( $v > 0.5$ ) or by consensus ( $v = 0.5$ ) or with veto ( $v < 0.5$ ).

If any one of the condition fails, then compromise solution is selected as follows.

- 1 Select alternatives  $a_1$  and  $a_2$  when Condition 2 is not met.
- 2 Select alternatives  $a_1, a_2, \dots, a_m$  satisfying each criteria when condition-1 is not met. The selection of  $a_m$  is based on the relation  $Q(a_m) - Q(a_1) < DQ$  for  $m$  close positions.

### 3.3 MOORA

‘Multi-objective optimisation based on ratio analysis’ (MOORA) method is developed by Brauers and Zavadskas (2006). It is one of the robust method of ranking and selecting the best optimum solution because it is unaffected by the weights of criteria.

Step 1 Construct the decision matrix and normalise it using equation (5).

Step 2 Add normalised performance values for benefit criteria. Similarly, add the normalised performance values for cost criteria [equations (17) and (18)].

$$B_i = \sum_{j=1}^g v_{ij}^* \tag{17}$$

$$C_j = \sum_{j=g+1}^m v_{ij}^* \tag{18}$$

where  $g$  denotes the number of beneficial criteria whereas  $(m - g)$  denotes the number of cost criteria.  $f_i$  represents the performance assessment number with reference to all the criteria involved for evaluation.

Step 3 Subtract the sum of cost criteria from benefit criteria for performance values using equation (19).

$$f_i = B_i - C_i \tag{19}$$

Step 4 Arrange all the performance assessment number in the decreasing order so as to obtain ordinal ranking of  $f_i$ . The highest value represents the best value corresponding to that alternative.

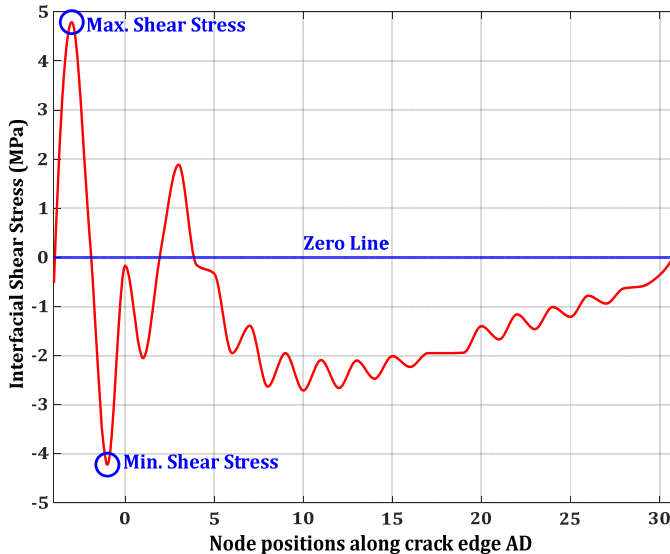
### 4 Results and discussion

Table 2 shows interfacial shear stress values at points A, B, C and D as shown in Figure 5 for 27 configurations. Configuration that exhibited a smooth distribution and minimum value of interfacial shear stress was chosen as the best one. Since this involves multiple criteria decision making; multi-criteria optimisation algorithms like TOPSIS, VIKOR and MOORA were implemented. These algorithms ranked every configuration on the basis of degree to which they satisfied both the criteria.

It was observed that the configuration no. 26; 600-600-300, achieved the first rank as reported by all the optimisation techniques. This configuration corresponds to the least values of interfacial shear stress and its fluctuation. Moreover, it represented the uniform distribution of the interfacial shear stress. Whereas the configuration no. 8 (200-600-300 ply) achieved the 26th, 24th and 25th rank for TOPSIS, VIKOR and MOORA respectively. This configuration was not recommended for the fatigue application as it showed the maximum interfacial shear stress values and also the maximum value of fluctuation. The second worse ply configuration was configuration no. 2 (200-200-300 ply), as it achieved the 27th and 26th rank by TOPSIS and MOORA respectively.

But VIKOR assigned the 7th preference to this configuration. Based on the rank observations, it was concluded that all three algorithms unanimously selected configuration no. 26 (600-600-300 ply) as the best configuration.

**Figure 6** Interfacial shear stress distribution for 600-600-300 (see online version for colours)



Graphical approach was utilised to visualise the nature of interfacial shear stress and its fluctuation for the best and the worst configurations respectively. For this purpose,

interfacial shear stress values were plotted along the crack edge AD to see the fluctuation patterns and the distribution of interfacial shear stress. One configuration with least fluctuations (600-600-300) and the other one with worst fluctuations (200-600-300) are discussed over here.

**Table 2** Interfacial shear stress and max. stress amplitude for all configurations with their rankings

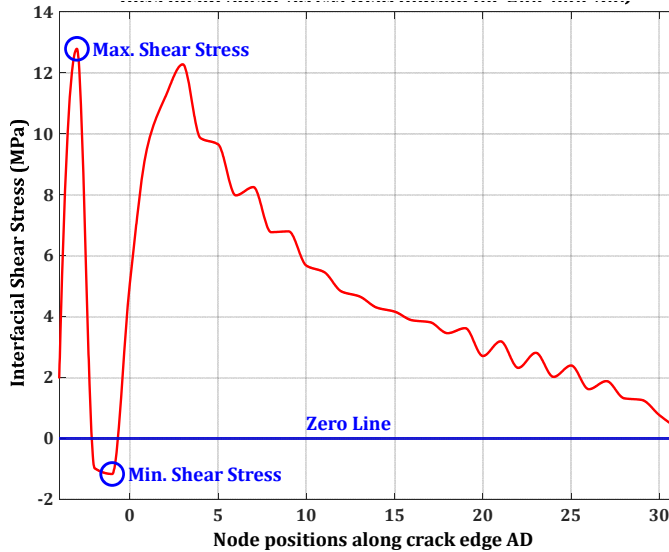
Sr. no.	Patch configuration for design of experiment	Interfacial shear stress (MPa)				Optimisation algorithms ranks		
		At A	At B	At C	At D	TOPSIS	VIKOR	MOORA
1	200-200-200	12.21	-1.58	11.25	0.27	25	20	22
2	200-200-300	11.28	-2.00	9.98	0.22	27	7	26
3	200-200-600	12.03	-1.53	11.11	0.27	18	21	17
4	200-300-200	11.22	-1.99	9.94	0.22	15	8	14
5	200-300-300	9.61	-2.68	7.92	0.14	7	6	7
6	200-300-600	11.06	-1.93	9.83	0.22	12	9	12
7	200-600-200	11.23	-1.95	10.27	0.24	16	17	16
8	200-600-300	12.79	-1.16	12.28	0.34	26	24	25
9	200-600-600	7.88	-3.40	5.58	0.34	5	5	5
10	300-200-200	12.17	-1.56	11.23	1.84	23	27	27
11	300-200-300	12.13	-1.55	11.21	0.28	21	22	19
12	300-200-600	11.07	-1.96	9.85	0.22	13	10	13
13	300-300-200	11.75	-2.05	10.50	0.25	22	11	21
14	300-300-300	11.72	-2.03	10.48	0.25	20	12	20
15	300-300-600	12.48	-1.20	11.78	0.32	24	23	23
16	300-600-200	12.36	-1.10	11.85	0.34	17	25	18
17	300-600-300	12.46	-1.11	12.06	0.34	19	26	24
18	300-600-600	5.27	-4.50	2.21	-0.13	4	4	4
19	600-200-200	11.16	-1.95	10.15	0.26	14	18	15
20	600-200-300	10.55	-1.83	9.52	0.23	11	13	11
21	600-200-600	10.43	-1.78	9.41	0.23	8	16	8
22	600-300-200	10.45	-1.80	9.44	0.23	10	14	10
23	600-300-300	10.44	-1.79	9.42	0.23	9	15	9
24	600-300-600	5.11	-4.47	2.12	0.14	3	3	3
25	600-600-200	4.81	-4.24	1.90	0.14	2	2	2
26	600-600-300	4.79	-4.22	1.89	0.14	1	1	1
27	600-600-600	9.37	-1.55	8.56	0.22	6	19	6

Figure 6 shows the interfacial shear stress distribution for 600-600-300 configuration. On X axis nodes are shown along the crack edge AD, whereas on Y axis values of interfacial shear stress are shown in MPa. Crack edge AD is shown in Figure 5. From the values mentioned in the Figure 6 it was concluded that compared to other configurations the

interfacial shear stress distribution has not shown any sudden spike in the value and also the values are much lower.

Similarly, the graphical representation of interfacial shear stress for configuration 200-600-300 is shown in Figure 7. It showed the presence of sudden spikes of large magnitude for the interfacial shear stress. The largest stress fluctuation was reported for this configuration; moreover, interfacial shear stress values are much higher. Because of this, it was not recommended for the practical application.

**Figure 7** Interfacial shear stress distribution for 200-600-600 (see online version for colours)



## 5 Conclusions

In this paper, two novel criteria were implemented instead of usual fracture toughness criteria. Interfacial shear stress and its fluctuation are responsible for the debonding tendency or peeling off tendency in the CFRP material when used for the restoration of cracked aluminium alloy plate. The debonding tendency was explored in detail with the help of three-layer ply of different thicknesses and different lengths. Full factorial design of experiment was conducted to identify the optimum configuration using custom designed fatigue testing machine. Multi-criteria optimisation techniques such as TOPSIS, VIKOR and MOORA were implemented to obtain anonymous ranking for the best configuration. These results were validated using finite element technique with the help of Abaqus 6.14. The graphical approach verified the results of multi-criteria optimisation.

Configurations 600-600-300, 600-600-200 and 600-300-600 showed no sign of debonding even after 1,500,000 fatigue cycles, while in other configurations debonding occurred after on an average of 80,000 fatigue cycles.

CFRP repairing is the best approach for cracked structures to extend their product life, however, they exhibit a tendency to debond (peeling off tendency). This debonding can be suppressed using a ply drop technique and placing plies of reducing lengths one above another. Lengths of plies decreases as the distance from the aluminium plate

increases. Experimental trials revealed that configuration 600-600-300 is the best combination for reducing debonding which can be used to repair the cracked wing structures of the aircraft as well as other structures which bears the fatigue load. In general, debonding can be avoided by keeping high density plies in the closer and middle layer, whereas medium density ply can be kept in the farthest layer from aluminium alloy plate.

## 6 Future scope of study

Real time monitoring of the structures which are in service helps to minimise the damage as well as the cost of the repair. This increases the product life. In this regard strain sensors can be attached to the CFRP and the displacement near the crack can be monitored while the structure is in service. The mechanism of this real time monitoring needs to be figure out along with the exact behaviour of CFRP when strain sensors are attached. Also, the strain sensors effect on strength of the structure needs to be studied in detail for different types of loading.

## References

- Ali, H.T., Fotouhi, S., Akrami, R., Pashmforoushd, F., Pavlovic, A. and Fotouhi, M. (2020) 'Effect of ply thickness on damage mechanisms of composite laminates under repeated loading', *FME Trans.*, Vol. 48, No. 2, pp.287–293, DOI: 10.5937/fme2002287t.
- Bachir Bouiadjra, B., Benyahia, F., Albedah, A., Bachir Bouiadjra, B.A. and Khan, S.M.A. (2015) 'Comparison between composite and metallic patches for repairing aircraft structures of aluminum alloy 7075 T6', *Int. J. Fatigue*, Vol. 80, pp.128–135, DOI: 10.1016/j.ijfatigue.2015.05.018.
- Baker, A.A. (1987) 'Fibre composite repair of cracked metallic aircraft components – practical and basic aspects', *Composites*, Vol. 18, No. 4, pp.293–308, DOI: 10.1016/0010-4361(87)90293-X.
- Bhaskar, S., Kumar, M. and Patnaik, A. (2020) 'Application of hybrid AHP-TOPSIS technique in analyzing material performance of silicon carbide ceramic particulate reinforced AA2024 alloy composite', *Silicon*, May, Vol. 12, No. 5, pp.1075–1084, DOI: 10.1007/s12633-019-00211-8.
- Brauers, W.K. and Zavadskas, E.K. (2006) 'The MOORA method and its application to privatization in a transition economy', *Control Cybern.*, Vol. 35, No. 2, pp.445–469.
- Cloud, G.L. (2016) 'Joining technologies for composites and dissimilar materials', *Proceedings of the 2016 Annual Conference on Experimental and Applied Mechanics*, Vol. 10, pp.1–10, <https://doi.org/10.1007/978-3-319-42426-2>.
- Eliasson, S., Wanner, S., Barsoum, Z. and Wennhage, P. (2019) 'Development of fatigue testing procedure for unidirectional carbon fiber composites', in *Procedia Structural Integrity*, January, Vol. 19, pp.81–89, DOI: 10.1016/j.prostr.2019.12.010.
- Gangwar, S., Yadav, S. and Pathak, V.K. (2021) 'Optimized selection of nanohydroxyapatite-filled dental restorative composites formulation for best physico-mechanical, chemical, and thermal properties using hybrid analytical hierarchy process-multi-objective optimization on the basis of ratio analysis approach', *Polym. Compos.*, DOI: 10.1002/pc.26097.
- Hwang, C-L. and Yoon, K. (1981) 'Methods for multiple attribute decision making', in *Multiple Attribute Decision Making. Lecture Notes in Economics and Mathematical Systems*, Vol. 186, Springer, Berlin, Heidelberg, [https://doi.org/10.1007/978-3-642-48318-9\\_3](https://doi.org/10.1007/978-3-642-48318-9_3).

- Kaliraj, M., Narayanasamy, P., Balasundar, P. and Rajkumar, M. (2017) 'Mechanical behaviour and analysis of advanced polymer-based Kevlar-49 composite material', *Int. J. Comput. Aided Eng. Technol.*, Vol. 9, No. 2, pp.251–260, DOI: 10.1504/IJCAET.2017.083397.
- Maharana, S.M., Pradhan, A.K. and Pandit, M.K. (2020) 'Performance evaluation of mechanical properties of nanofiller reinforced Jute-Kevlar hybrid composite', *J. Nat. Fibers*, DOI: 10.1080/15440478.2020.1777246.
- Mohan, P., Azhagesan, N. and Sivapragash, M. (2018) 'The preparation and mechanical properties of Al metal matrix composites by in-situ method', *Int. J. Comput. Aided Eng. Technol.*, Vol. 10, Nos. 1/2, p.35, DOI: 10.1504/IJCAET.2018.10009680.
- Moradi, A., Leguillon, D. and Carrère, N. (2013) 'Influence of the adhesive thickness on a debonding – an asymptotic model', *Eng. Fract. Mech.*, Vol. 114, pp.55–68, DOI: 10.1016/j.engfracmech.2013.10.008.
- Opricovic, S. and Tzeng, G.H. (2004) 'Compromise solution by MCDM methods: a comparative analysis of VIKOR and TOPSIS', *Eur. J. Oper. Res.*, July, Vol. 156, No. 2, pp.445–455, DOI: 10.1016/S0377-2217(03)00020-1.
- Ouinass, D., Bachir Bouiadjra, B., Himouri, S. and Benderdouche, N. (2012) 'Progressive edge cracked aluminium plate repaired with adhesively bonded composite patch under full width disbond', *Compos. Part B Eng.*, Vol. 43, No. 2, pp.805–811, DOI: <https://doi.org/10.1016/j.compositesb.2011.08.022>.
- Pandey, P. and Kumar, S. (2010) 'Adhesively-bonded patch repair with composites', *Def. Sci. J.*, March, Vol. 60, pp.320–329, DOI: 10.14429/dsj.60.360.
- Papanikos, P., Tserpes, K.I. and Pantelakis, S. (2007) 'Initiation and progression of composite patch debonding in adhesively repaired cracked metallic sheets', *Compos. Struct.*, Vol. 81, No. 2, pp.303–311, DOI: 10.1016/j.compstruct.2006.08.022.
- Patil, M.V. (2017) 'Multi-response simulation and optimization of gas tungsten arc welding', *Appl. Math. Model.*, February, Vol. 42, pp.540–553, DOI: 10.1016/j.apm.2016.10.033.
- Patil, M.V. and Kulkarni, A.J. (2020) 'Pareto dominance based multiobjective cohort intelligence algorithm', *Inf. Sci. (Ny)*, October, Vol. 538, pp.69–118, DOI: 10.1016/j.ins.2020.05.019.
- Patterson, W. and Force, A. (1976) 'The Halpin-Tsai equations: a review', *Polymer Engineering & Science*, Vol. 16, No. 5, pp.344–352, <https://doi.org/10.1002/pen.760160512>.
- Raj, S.S., Pradeep, P. and Dhas, J.E.R. (2021) 'Parameter optimisation of a fibre reinforced polymer composite by RSM design matrix', *Int. J. Comput. Aided Eng. Technol.*, Vol. 15, Nos. 2/3, p.375, DOI: 10.1504/IJCAET.2021.117134.
- Ramji, M. and Srilakshmi, R. (2012) 'Design of composite patch reinforcement applied to mixed-mode cracked panel using finite element analysis', *J. Reinf. Plast. Compos.*, Vol. 31, No. 9, pp.585–595, DOI: 10.1177/0731684412440601.
- Rice, J.R. (1967) *Division of Engineering The Approximate Analysis of Strain Concentration by Notches and Cracks*, Department of Defense Advanced Research Projects Agency Contract SD-86 Material Research Program ARPA SD-86 Report E39, May.
- Sadhasivam, R.M.S., Ramanathan, K., Sargunanathan, S. and Manikandan, M. (2021) 'A study on the machinability behaviour of Al6061-ZnO(p) metal matrix composite through wire-cut electro discharge machining using multi-objective optimisation on the basis of ratio analysis', *Int. J. Comput. Aided Eng. Technol.*, Vol. 15, Nos. 2/3, p.385, DOI: 10.1504/IJCAET.2021.117141.
- Saravanan, S. and Ganesan, K. (2017) 'Mechanical testing of epoxy bonded eco friendly natural fibre composite material', *Int. J. Comput. Aided Eng. Technol.*, Vol. 9, No. 2, pp.241–250, DOI: 10.1504/IJCAET.2017.083396.
- Srilakshmi, R., Ramji, M. and Chinthapenta, V. (2015) 'Fatigue crack growth study of CFRP patch repaired Al 2014-T6 panel having an inclined center crack using FEA and DIC', *Eng. Fract. Mech.*, Vol. 134, pp.182–201 [online] <https://doi.org/10.1016/j.engfracmech.2014.12.012>.

- Srivastava, S., Kumar, S. and Garg, R.K. (2021) 'A multi-objective optimisation of TIG welding parameters using response surface methodology', *Int. J. Comput. Aided Eng. Technol.*, Vol. 14, No. 4, pp.575–590, DOI: 10.1504/IJCAET.2021.115363.
- Suresha, B. and Saini, M.S. (2018) 'Fabrication and mechanical characterisation of carbon fabric reinforced epoxy with alumina and molybdenum disulfide fillers', *Int. J. Comput. Aided Eng. Technol.*, Vol. 10, Nos. 1/2, p.89, DOI: 10.1504/IJCAET.2018.10009684.
- Tamboli, S., Pandey, A., Bongale, A. and Kumar, S. (2019) 'Performance evaluation of cracked aluminum alloy repaired with carbon fiber reinforced polymer for aerospace application', *Mater. Res. Express*, Vol. 6, No. 11, DOI: 10.1088/2053-1591/ab493c.
- Thirukumaran, M., Kannan, L.V. and Sankar, I. (2018) 'Study on mechanical properties of glass wool/epoxy reinforced composite', *Int. J. Comput. Aided Eng. Technol.*, Vol. 10, Nos. 1/2, p.15, DOI: 10.1504/IJCAET.2018.10009678.
- Vavrik, D. and Jandejsek, I. (2014) 'Experimental evaluation of contour J integral and energy dissipated in the fracture process zone', *Eng. Fract. Mech.*, Vol. 129, pp.14–25, DOI: 10.1016/j.engfracmech.2014.04.002.
- Venkategowda, C., Rajanna, S., Udupa, N.G.S. and Keshavamurthy, R. (2018) 'Experimental investigation of glass-carbon/epoxy hybrid composites subjected to low velocity impact test', *FME Trans.*, Vol. 46, No. 4, pp.595–602, DOI: 10.5937/fmet1804595R.
- Vignesh, V. and Kumar, S.S. (2022) 'Effect of titanium oxide, alumina oxide and silicon carbide on mechanical properties and thermal properties of reinforced nylon composites for industrial applications', *Int. J. Comput. Aided Eng. Technol.*, Vol. 16, No. 1, p.1, DOI: 10.1504/ijcaet.2022.10032090.
- Zhu, X-K. and Joyce, J.A. (2012) 'Review of fracture toughness (G, K, J, CTOD, CTOA) testing and standardization', *Eng. Fract. Mech.*, Vol. 85, pp.1–46, DOI: <https://doi.org/10.1016/j.engfracmech.2012.02.001>.